

CHROM. 19 224

CAPILLARY ISOELECTRIC FOCUSING

EFFECTS OF CAPILLARY GEOMETRY, VOLTAGE GRADIENT AND ADDITION OF LINEAR POLYMER

WOLFGANG THORMANN*, AMOS TSAI, JON-PIERRE MICHAUD, RICHARD A. MOSHER and MILAN BIER

Center for Separation Science, University of Arizona, Bldg. 20, Tucson, AZ 85721 (U.S.A.)

(First received September 4th, 1986; revised manuscript received October 31st, 1986)

SUMMARY

Free-fluid focusing of both simple buffer and Ampholine systems in various capillaries of rectangular cross-sections was investigated by following the temporal behavior of the current under constant voltage and the transient double peak approach to equilibrium of colored test proteins. For systems comprising two and three buffer constituents the ratio of initial to final focusing current compares well with data obtained by computer simulation. Experiments have also been performed in the presence of linear, non-crosslinked polyacrylamide to assess its fluid stabilizing potential in capillaries. Good focusing and resolution are commensurate with a high initial to final current ratio, no substantial drifts after separation (attainment of steady state) and proper boundary conditions at both column ends. The production of turbulent protein foci at high-voltage gradients is discussed with the aid of electric field profiles monitored along the focusing column.

INTRODUCTION

Isoelectric focusing (IEF) in gel-filled capillaries of 5–20 μ l volume provides high-resolution analyses of microamounts of complex protein mixtures¹. The principle and feasibility of free solution IEF in capillaries has been investigated by Thormann and co-workers^{2–4} employing a 10-cm capillary of rectangular shape. Our approach allows the dynamics of the electric field to be followed during focusing via the use of a linear array of potential gradient sensors². In conjunction with computer simulation data, this has enabled the focusing mechanism of *n* component systems to be elucidated³. The data illustrate the existence of two phases in IEF, a relatively fast separation phase which is followed by a slow stabilizing phase during which the theoretical steady state is attained. The production of conductance gaps in synthetic mixtures of carrier ampholytes has also been visualized which allows the different mixtures in use to be characterized and compared⁴. In these mixtures a cathodic drift of the position of lowest conductivity was monitored. Free-fluid IEF has also been

examined by Hjertén and Zhu⁵ using a 12-cm glass capillary of 0.2 mm I.D. In this apparatus proteins were detected by on- or off-capillary measurements of their UV absorbance⁵ using stationary optical microcells. This required the proteins to be mobilized following the focusing process. In comparison to IEF in gel-filled capillaries the free-fluid approach permits on-line detection of solutes, simpler procedures for column filling and cleaning, and is therefore more attractive from the point of view of automation of the procedure.

In this communication we wish to report the results of our investigations using various geometries of the focusing trough. Some of the experimental data are compared with computer simulation data which were obtained using the generalized, dynamic model of Bier *et al.*⁶. The influence of linear polyacrylamide on the degree of focusing in capillaries is also discussed as are the conditions for establishment of turbulent protein foci in steplike pH gradients.

MATERIALS AND METHODS

Instrumentation

The CapScan apparatus featuring a linear potential gradient array detector along the focusing column² was used for most of the experiments described in this paper. A schematic representation of the focusing cell, including the thermostated aluminum slab (A), an electrode bearing glass plate (B), a silicone gasket (C), a plexiglass block (D) and the electrode compartments (E), is shown in Fig. 1a. It comprises a 10-cm capillary column with rectangular cross section between points 1 and 3 and two small cylindrical sections with a diameter of 1 mm [between points 1 and 3 respectively and the membranes (7)]. The dimension of the rectangular part is defined by the silicone gasket (C). Its thickness and the shape of the channel (see Fig. 1c) provide a wide flexibility in achieving focusing troughs of various cross sectional areas. Sheet silicone material of 0.2–2.4 mm thickness was used for the two columns having widths of 1–2, and 15 mm respectively as depicted in Fig. 1c. PTFE of 0.3 mm thickness was also used. The channel was cut into the gasket employing a scalpel together with a template made from 1 mm thin aluminum.

The small dimensions of the capillary enables sharp focusing in free solution. Dialysis membranes (7) define both ends of the focusing column and isolate the electrode compartments from the trough. Disks of 5-mm radii (7) were mounted with two silicone gaskets (18, 19) and a membrane holder made from Delrin (4) as shown schematically in Fig. 1b. If not otherwise stated, small amounts of sodium hydroxide and orthophosphoric acid, 0.1 *M* each, were the respective cathodic and anodic electrolytes employed. A Kepco Power Supply APH 2000M or a home-made voltage stabilized unit were used.

In a capillary of the CapScan with the dimensions 0.63 × 2.0 × 100 mm, as well as in 7.5 cm long glass tubes of 2.2 and 1.16 mm I.D. mounted between two simple electrode housings, comparison experiments were performed with the addition of linear, non-crosslinked polyacrylamide (LPA). LPA solutions of 60 ml were prepared through rapid (1 h, 50°C) polymerization of 10% acrylamide (Bio-Rad Labs.) containing 0.36 ml N,N,N',N'-tetramethylethylenediamine (TEMED) (Bio-Rad Labs.) and 0.18 ml 25% ammonium persulfate (Sigma). No crosslinking agent, such as bisacrylamide, was included. The product was kept overnight at room temperature

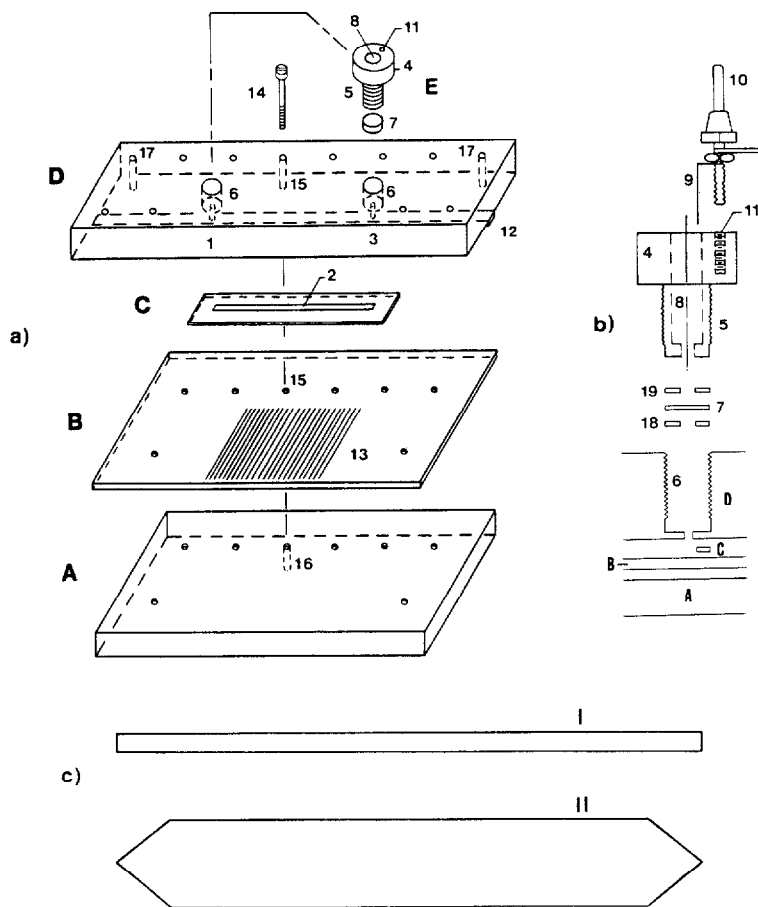


Fig. 1. Schematic representations of exploded assembly of the CapScan capillary IEF separation cell (a), the electrode assembly (b) and the focusing troughs employed (c). A = Thermostated aluminum plate; B = sensor bearing glass plate; C = silicone rubber gasket; D = block of plexiglass; E = electrode compartments; 1-3 = separation trough; 4 = membrane holder with electrode compartment; 5 = thread for mounting of membrane holder; 6 = threaded hole in plexiglass block; 7 = membrane; 8 = electrode compartment; 9 = platinum electrode; 10 = banana plug for power connection; 11 = threaded hole for mounting of banana plug; 12 = sealing edge; 13 = detection electrodes; 14 = mounting screw; 15 = screw hole; 16 = threaded hole; 17 = screw hole for cell attachment to the scanner (not shown); 18 and 19 = ring-shaped silicone gasket; I = column I having a width of 1-2 mm; II = column II with a width of 15 mm. Not shown in these figures are the power supply, the mechanical scanner and the computer system. For a block diagram of the entire CapScan system see ref. 4.

followed by precipitation of LPA in ethanol (three times in 1-liter aliquots), drying at 40°C and redissolution in water in order to achieve a desired w/v ratio. The purification reduced absorption at 280 nm from 0.2 to *ca.* 0.02. The LPA was diluted 1 to 2 with an aqueous solution containing carrier and test components. A disposable syringe was used to insert the highly viscous solution into the focusing capillary.

TABLE I
PROPERTIES OF ELECTROLYZED BUFFER SOLUTIONS

Composition	Concentration (mM)	pH*		Conductivity* (mS/cm)	
		<i>m</i>	<i>c</i>	<i>m</i>	<i>c</i>
glu, his	15, 15	5.23	5.16	0.645	0.771
glu, cser	15, 15	4.37	4.35	0.472	0.526
glu, his, arg	10, 10, 10	7.47	7.41	0.469	0.533
glu, cser, arg	10, 10, 10	5.95	6.02	0.504	0.539
glu, cser, his	10, 10, 10	5.36	5.35	0.443	0.547

* *m* = Measured values using conventional equipment; *c* = calculated values with conditions given in Table II.

Chemicals and experimental procedure

Various two- and three-component buffer mixtures (Table I) were produced using analytical grade chemicals as available. Bromphenol blue stained human serum albumin ($pI = 4.8$) and human hemoglobin ($pI = 7.3$) were focused in these systems, as well as in a 1% solution of wide pH range (3.5–10) Ampholine (LKB, Bromma, Sweden). The properties of the solutions are given in Table I. All experiments commenced with a homogeneous mixture of carrier and test constituents. The focusing process was characterized by monitoring three parameters. First, the focusing current was measured under constant voltage. The temporal behavior of the current as well as the ratio between initial and final (steady state) currents was used as a measure of the focusing degree achievable in a given assembly. Secondly, the two colored proteins in the sample were followed photographically and thirdly the electric field profiles were monitored as previously described^{3,4}.

Computer predictions

The dynamic computer model of Bier *et al.*⁶ was used to simulate the change of total resistance during focusing of simple buffer mixtures. The one dimensional approach assumes the absence of convective flows and thermal gradients and computes concentration, pH and conductivity at a specified number of grid points along the focusing axis for given initial conditions and applied current. The assumption is also made that the current across the end plates is carried by hydroxyl and hydronium ions only. The conditions employed are summarized in Table II.

RESULTS AND DISCUSSION

Characterization of the focusing degree in capillary columns

The temporal behavior of the focusing current for various buffer solutions and Ampholine is presented in Fig. 2a. The CapScan apparatus with a 0.5 mm thick silicone gasket, a 1 mm wide channel (Fig. 1c) and dialysis membranes was used. In all cases the current decreases substantially until reaching equilibrium. The corresponding ratios of initial to final current are listed in Table III together with those

TABLE II
CONDITIONS FOR COMPUTER SIMULATIONS

<i>General values</i>			
Column length	1 cm		
Segmentation	100 segments/cm		
Current density	0.001 A/cm ²		
<i>pK_a and mobility values</i>			
<i>Component</i>	<i>pK_{a1}</i>	<i>pK_{a2}</i>	<i>Mobility × 10⁴ (cm²/Vs)*</i>
Glutamic acid	2.16	4.29	2.97
Cycloserine	4.40	7.40	3.42
Histidine	6.02	9.17	2.85
Arginine	9.04	12.48	2.26
H ₃ O ⁺			36.27
OH ⁻			19.87

* It was assumed that all species of a component have equal mobility coefficients.

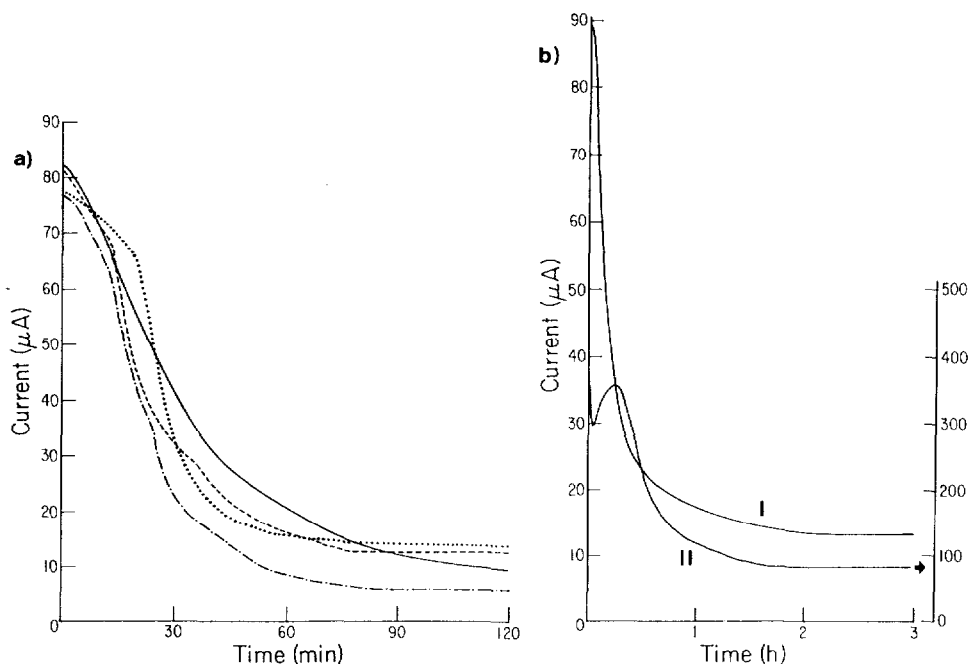


Fig. 2. (a) Variation of focusing current for different electrolytes under constant voltage of 300 V using column I with a width of 1 mm. The column height was about 0.5 mm. 1% of pH 3.5–10 Ampholine (solid line); glutamic acid, cycloserine, arginine (10 mM each, dotted line); glutamic acid, cycloserine, histidine (10 mM each, dashed line); cacodylic acid, histidine, Tris (8.76, 7.05, and 8.27 mM respectively³, hybrid line). (b) Variation of current during focusing of glutamic acid and histidine (15 mM each) in columns I (left axis) and II (right axis) with a 0.5-mm silicone gasket. The applied voltage was 150 V in both cases.

TABLE III
EXPERIMENTAL* AND THEORETICAL** FOCUSING DATA

System	Experimental data with 0.5-mm gasket***		Computer prediction
	Column I (1 mm)	Column II (15 mm)	
glu, his	7.5	4.5 (4.8)	8.9
glu, cser	4.3 (5.8)	(3.4)	4.9
glu, his, arg	7.8	—	8.9
glu, cser, arg	6.0 (6.2)	2.5 (3.0)	6.8
glu, cser, his	6.5	—	8.0

* Initial to final current ratio under constant voltage.

** Ratio of final to initial resistance across total column.

*** The numbers in parentheses indicate the current ratio in presence of about 0.23 mg/ml bromphenol blue stained human serum albumin. Dialysis membranes at the column ends were used.

obtained from the mathematical model. The theoretical ratio of final to initial resistance represents an idealized, isothermal situation and provides a comparative value to the experimentally determined ratio of initial to final focusing current under constant voltage. Its accuracy is dependent upon the accuracy of the electrophoretic mobilities and pK values used. However, in all configurations the experimental data are lower than the theoretical which may be attributed to electroosmosis and residual density-driven convection within the capillary and the electrode assembly. It is interesting to note that the current ratio increases with the presence of test proteins (Table III) which is due to the production of highly non-conducting protein foci. In summary, the experimental and the theoretical data compare well indicating minimized convective disturbances in column I. As reported previously³ there is also good consistency between the experimental results of the dynamics of simple three-component model mixtures and the corresponding computer prediction.

It has been reported that good focusing is commensurate with a high ratio of initial to final current⁷. Studies undertaken with a range of cross sectional areas of the rectangular capillary revealed that the current ratio decreases with increasing cross section. For example, the focusing of glutamic acid, cycloserine and histidine (10 mM each) with silicone gasket thicknesses of 0.25, 0.5 and 1.6 mm provided current ratios of 7.1, 6.5 and 5.1, respectively (column I of Fig. 1c with 1 mm width; dialysis membranes). Slumping of focused protein zones⁷ was observed with column heights (thickness) > 0.6 mm making this configuration unfeasible for high-resolution separations. A rectangular electrophoresis capillary of the kind used in this work loses its thermostatic performance with increasing height, as was reported for capillary isotachopheresis⁸. Thus the height of this 1 mm width channel should be no greater than 0.5 to insure good focusing. A substantial decrease of the current ratio was also found with increasing channel width. Solutions of 1% Ampholine revealed ratios of 9.1 and 6.3 with widths of 1 and 2 mm respectively and a silicone gasket thickness of 0.5 mm.

The thin ribbonlike column with much higher aspect ratio (column II of Fig. 1c) was used to gain further insight into the impact of the channel width. The current

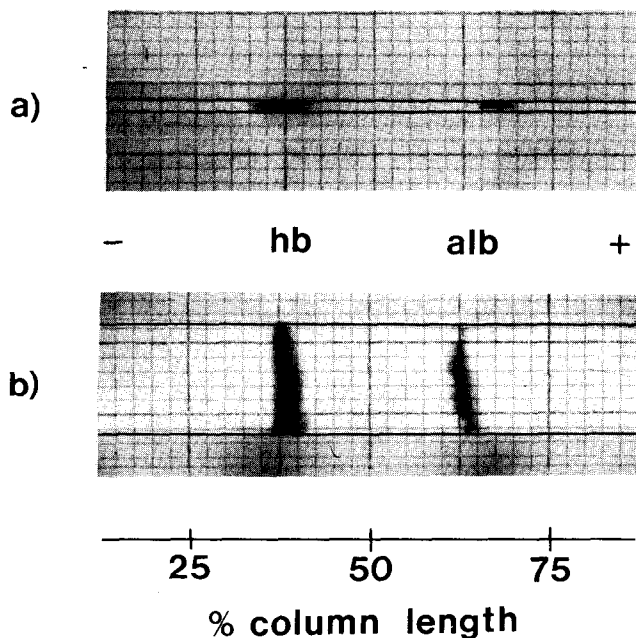


Fig. 3. Photographs of focused blue stained, human serum albumin (alb) and hemoglobin (hb) in troughs I (a) and II (b). The column dimensions are the same as used for Fig. 2b. The buffer solution was composed of glutamic acid, cycloserine and arginine (10 mM each) and contained human serum albumin and hemoglobin, 0.25% each. The applied voltage was 150 V and the steady-state currents were 8 μ A (a) and 115 μ A (b) respectively.

ratios for a number of two and three component buffer mixtures listed in Table III, are significantly lower than those in the narrower trough. Fig. 2b compares the current-time relationship during electrolysis in both columns. In column I the current drops gradually before reaching equilibrium whereas in the thin, ribbonlike channel of 15 mm width the current decreases first for a short time only, followed by a sudden increase to a maximum value and a decrease to its steady state value. As is summarized in Table III, the substantially smaller current ratios of column II as compared to column one indicate less fluid stability in the wide trough. The photographs shown in Fig. 3 depict typical results for both columns. It is interesting to note that the thin-film configuration is very sensitive to levelling. If not completely horizontal, the focused proteins accumulate on the lower side due to the large density gradient. The viscosity alone is not capable of completely stabilizing the quiescent fluid layer. It is well known, however, that laminar flow of electrolyte through a thin ribbonlike channel will provide sufficient stability, and allows successful separations in continuous flow electrophoresis⁹ and field flow fractionation¹⁰.

Electrode assemblies at the column ends are known to have an impact on the steady-state pattern produced¹¹. Instead of using dialysis membranes, ion-exchange membranes or non-gassing palladium electrodes can be employed for the isolation of the focusing trough from the electrode compartments. The different electrode assemblies do not alter the separation scheme in IEF but do change the length of the focused zone pattern as will be described in detail elsewhere¹².

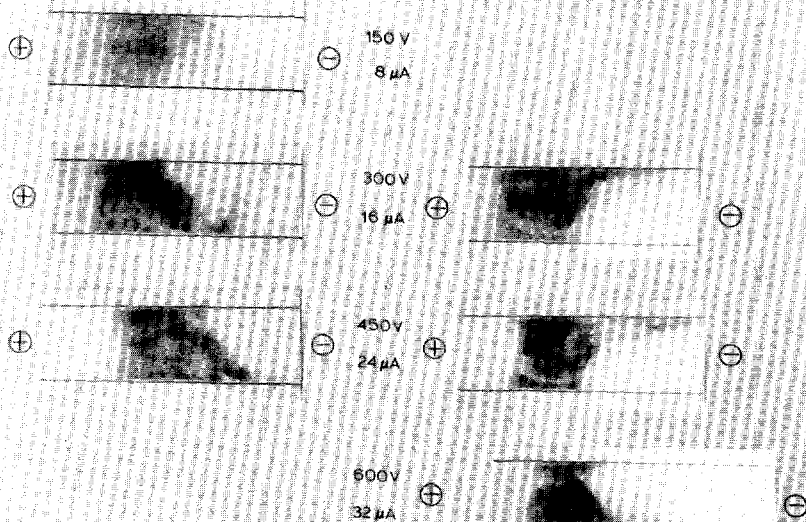


Fig. 4. Photographs of bromphenol blue stained albumin focused in the step pH gradient between glutamic acid and cycloserine (column I). The pictures were taken from a video screen after taking a video movie of the protein spot at various current densities. The increasing production of protein waves along the column wall is clearly seen at increasing currents. A mixture of glutamic acid and cycloserine (15 mM each) with 0.34 mg albumin per ml solution was focused at 300 V. The total column volume was about 80 μ l.

Voltage gradient

Both speed of separation and resolution in IEF are directly proportional to the voltage gradient and are thus a function of the efficiency with which the Joule heat is removed. Instrumental parameters, such as the removal of the generated heat, define the upper limit of the electric field which can be applied. Hjertén and Zhu⁵ have shown in their focusing glass tube with the dimensions 120 mm \times 0.2 mm I.D. \times 0.4 mm O.D. that complete focusing could be achieved within about 15 min. These short run times could be obtained because of rapid removal of the Joule heat through the thin glass walls, allowing the application of 1000 to 3000 V with current densities in the order of 0.2 A/cm². During most of our investigations with the CapScan apparatus a lower current density of 0.02 to 0.05 A/cm² was applied (10–50 V/cm) leading to focusing times in the order of 1 h and allowing the elucidation of the detailed focusing dynamics^{3,4}. However, field strengths matching those of Hjertén and Zhu could also be used in systems comprising Ampholine (500 V/cm). Dealing with steplike pH gradients established between simple buffer components, however, does not allow the application of such high driving fields. Our investigations revealed the existence of turbulent protein zones at moderate voltage gradients. Fig. 4 presents photographs of an albumin focus between glutamic acid and cycloserine (column I), showing a range of protein distributions at various currents. The pictures were taken

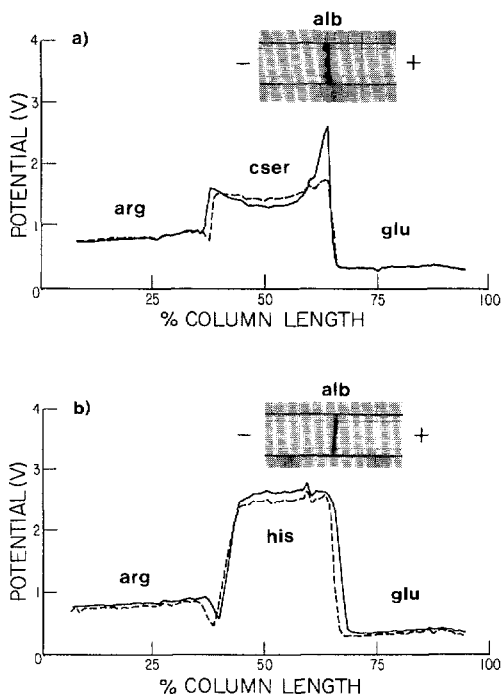


Fig. 5. Electric field profiles across the steady-state distribution of glutamic acid, cycloserine and arginine (a) and glutamic acid, histidine and arginine (b). The initial concentration of each buffer constituents was 10 mM. The anode is to the right. The dashed lines represent the plain carrier electrolyte, whereas the solid lines depict the electric field distribution in presence of an albumin focus (23 μ g) in the glutamic acid–cycloserine boundary (a) and in the glutamic acid–histidine boundary interface (b). The profiles were monitored at a constant current of 10 μ A using column I. The inserts depict corresponding foci of human serum, bromphenol blue stained albumin established in column II. The applied voltage was 150 V in both cases. The steady state currents were 120 μ A (a) and 114 μ A (b).

from a video screen after the movements of the protein were monitored with a video camera. According to theoretical considerations the width of a focused protein zone should be indirectly related to the current density^{13,14}. This prediction is based on an isothermal system with no convective mixing. In free solution, this relationship does not apply if the current density is equal to or above a threshold value specific for the system in use.

Fig. 5 shows monitored electric field profiles across the two three-component systems without protein (dashed line) and with albumin focused in the more anodic transition (solid line). The boundaries between each pair of amino acids are marked by a sudden change of the electric field. The protein focuses nicely in the two gradients as documented with the inserted photographs. Albumin at this concentration was found to be interactive with the buffer components of the glutamic acid–cycloserine boundary, whereas the electric field profile does not change in the other system. In this case the low conductivity of the focused protein zone is masked by the high electric field strength within the histidine zone.

The albumin focus within the glutamic acid–cycloserine boundary was found to be the point of lowest conductivity along the focusing column (Fig. 5a). It was a point of instability which exhibited eruptions during which protein was thrown along one side wall into the zone of pure cycloserine. This phenomenon was found to be very dynamic since equilibrium was quickly restored and the system awaited the next eruption which usually occurred along the other side wall. Above a certain plateau value the intensity and frequency of these events increased dramatically with increasing voltage gradient, and reaching a state of complete turbulence. The threshold value for the glutamic acid–cycloserine boundary was found to be significantly lower than that of the glutamic acid–histidine boundary where no turbulence was seen below 200 μA . The turbulent protein foci were observed in both columns as is documented with the photographs presented in Figs. 4 and 5. With a wide channel several points of instability were produced in the lateral column dimension. A very similar observation was made in continuous flow and free fluid recycling focusing⁹, manifested by the periodic eruption of the focused protein while travelling through the separation cell, producing a comb-like, frayed-out protein line^{15,16}. In summary, the combined effects of local electroosmosis and thermal instability, both driven by the high electric field, contribute to the observed protein foci.

Viscosity increase through inclusion of linear polymers

From the results seen so far in our laboratory and elsewhere, resolution in gels remains better than in free-fluid capillary IEF, even if columns with cross sectional areas as small as 0.01 mm² are used. A further decrease of the column dimensions would be feasible but not without sacrificing the ease of simple on-line detection. We were therefore searching for a medium which (i) minimizes convective flows in capillaries of the above mentioned dimensions, (ii) is a fluid, (iii) is optically transparent between 800 and 200 nm, and (iv) does not interfere with the focusing process. Linear, non-crosslinked polyacrylamide in the concentration range of 4 to 20% and with various chain-lengths was used to substantially increase the viscosity of the focusing solution. Fig. 6 presents the temporal behavior of the current for a 1% w/v Ampholine system in free solution (a) and with 5% LPA (b) containing hemoglobin and albumin. The applied voltage was a constant 150 V. The currents in both cases decreased substantially as focusing progressed yielding current ratios of 6.6 and 9.9 respectively. Fig. 6c and d depicts photographs of the focused test proteins in the two configurations. LPA clearly increases the anticonvectiveness of the medium within the capillary of 0.63 \times 2.0 mm cross-section as is manifested with the sharper foci in Fig. 6d. In other reports LPA was also shown (i) to reduce electroosmosis in agarose gels¹⁷, (ii) to provide a medium with molecular sieving characteristics in zone electrophoresis¹⁸, (iii) to increase the mechanical stability of large pore acrylamide gels¹⁹ and (iv) to serve as conductivity and electroosmosis quencher for IEF in immobilized pH gradients at acidic and alkaline extremes²⁰.

There are a number of disadvantages in conjunction with LPA containing electrolytes including the restriction to optical measurements at wavelengths $>$ 270 nm (Fig. 6e) and the difficult handling of solutions containing more than 1% LPA. The relatively small decrease in viscosity of an LPA solution with increased temperature excludes an effective use of temperature programming for fluid handling. Preliminary results from our laboratory indicate, however, that this can be overcome

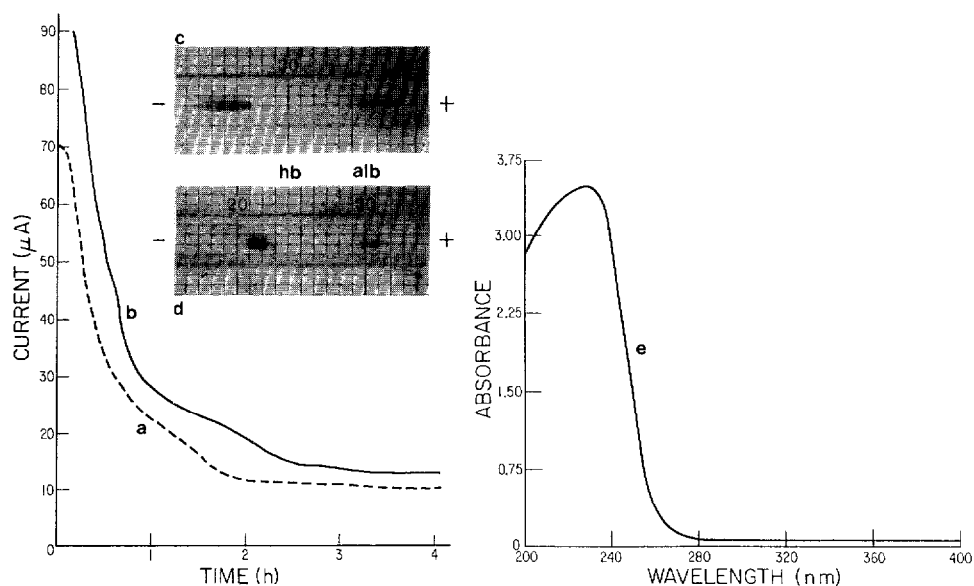


Fig. 6. Variation of focusing current in free fluid (a) and in a 5% LPA containing medium (b) during electrolysis of 1% Ampholine (pH 3.5–10) under a constant 150 V. The two photographs depict focused human serum albumin (alb) and hemoglobin (hb) in free solution (c) and 5% LPA (d). The UV spectrum (e) illustrates the sharp cutoff of LPA around 260 nm.

with LPA–agarose mixtures which are characterized by a more significant change in viscosity as function of temperature. Fluid insertion and capillary rinsing at 50°C followed by a run at room temperature provided good focusing results. Also, the presence of LPA was found to induce an undesired drift of the whole zone pattern towards the cathode. The drift was small in the capillary of rectangular shape but pronounced in the glass tube apparatus. In these tubes with fairly high internal diameter conical zones indicating an appreciable axial temperature profile evolved quickly and resolved into the steady-state protein zones which looked like arrow heads. This is consonant with the findings of Tietz *et al.*¹⁸ who observed diffuse tongues at the center of electrophoretic tubes instead of discrete bands. The glass tube configuration is less attractive than that with the capillary of the CapScan apparatus where three different surfaces (glass, plexiglass and silicone) with unequal zeta potentials are present. On the other hand procedures to decrease surface charge of glass capillaries are well known²¹ and could be used in conjunction with LPA.

CONCLUSIONS

Experiments reported here and elsewhere^{2–5,12} provide the basis for free-fluid capillary IEF. The feasibility, the boundary conditions and basic limitations are fully recognized. They indicate the limiting parameters in terms of cross-sectional area, voltage gradient, electrode assembly, increase of viscosity through the addition of a neutral polymer and surface properties of capillary walls. On-line detection of solutes during and after focusing in our present capillary devices is difficult except when the

protein changes the local electric field. The approach chosen by Hjertén and Zhu requires the mobilization of the focused proteins in order to monitor them while they migrate across a specified location. An optical (UV–VIS) absorbance–fluorescence detector adapted for rapid movements along the capillary, a linear array of a fiber optics or a linear array of optical, solid-state sensing probes²² would provide the logical advancement to make capillary IEF a more practical methodology. Computer aided data collection, storage and processing would complete this approach towards a fully instrumental scheme for which tedious staining procedures of the solutes of interest could be avoided.

ACKNOWLEDGEMENTS

The authors would like to acknowledge valuable discussions with Dr. N. B. Egen, the video recordings with Dr. J. Kessler and the experimental assistance of L. Zawadski. This work was supported in part by NASA grants NSG-7333 and NAGW-693, by NSF grant CPE-8311125 and by a grant from the Swiss National Science Foundation.

REFERENCES

- 1 V. Neuhoff, *GIT Fachz. Lab.*, 8 (1984) 649 [or *Funkt. Biol. Med.*, 1 (1982) 1] and references cited therein.
- 2 W. Thormann, G. Twitty, A. Tsai and M. Bier, in V. Neuhoff (Editor), *Electrophoresis '84*, Verlag Chemie, Weinheim, 1984, pp. 114.
- 3 W. Thormann, R. A. Mosher and M. Bier, *J. Chromatogr.*, 351 (1986) 17.
- 4 W. Thormann, N. B. Egen, R. A. Mosher and M. Bier, *J. Biochem. Biophys. Methods*, 11 (1985) 287.
- 5 S. Hjertén and M.-D. Zhu, *J. Chromatogr.*, 346 (1985) 265.
- 6 M. Bier, O. A. Palusinski, R. A. Mosher and D. A. Saville, *Science (Washington, D.C.)*, 219 (1983) 1281.
- 7 N. B. Egen, G. E. Twitty, W. Thormann and M. Bier, *Sep. Sci. Technol.*, in press.
- 8 Z. Ryšlavý, P. Boček, M. Deml and J. Janák, *J. Chromatogr.*, 144 (1977) 17.
- 9 M. Bier, N. B. Egen, G. E. Twitty, R. A. Mosher and W. Thormann, in C. J. King and J. D. Navratil (Editor), *Chemical Separations, Vol. 1, Principles*, Litarvan Literature, Denver, CO, 1986, pp. 133.
- 10 J. C. Giddings, *Sep. Sci. Technol.*, 19 (1984–1985) 831.
- 11 N. Y. Nguyen and A. Chrambach, *Anal. Biochem.*, 82 (1977) 54.
- 12 R. A. Mosher and W. Thormann, *J. Chromatogr.*, in preparation.
- 13 E. Schumacher, *Helv. Chim. Acta*, 40 (1957) 2322.
- 14 O. A. Palusinski, A. Graham, R. A. Mosher, M. Bier and D. A. Saville, *AIChE J.*, 32 (1986) 215.
- 15 H. Wagner and G. E. Twitty, personal communications.
- 16 R. E. Manzoni, *PhD. Dissertation*, Universität des Saarlandes, Saarbrücken, 1985.
- 17 B. G. Johansson and S. Hjertén, *Anal. Biochem.*, 59 (1974) 200.
- 18 D. Tietz, M. H. Gottlieb, J. S. Fawcett and A. Chrambach, *Electrophoresis*, 7 (1986) 217.
- 19 N. C. Mills and J. Ilan, *Electrophoresis*, 6 (1985) 531.
- 20 R. A. Mosher, M. Bier and P. G. Righetti, *Electrophoresis*, 7 (1986) 59.
- 21 S. Hjertén, *J. Chromatogr.*, 347 (1985) 191.
- 22 W. Thormann, *J. Chromatogr.*, 334 (1985) 83.